

Enhanced direct flexoelectricity in paraelectric phase of Ba(Ti_{0.87}Sn_{0.13})O₃ ceramics

Longlong Shu, Xiaoyong Wei, Li Jin, Yong Li, Hong Wang et al.

Citation: *Appl. Phys. Lett.* **102**, 152904 (2013); doi: 10.1063/1.4802450

View online: <http://dx.doi.org/10.1063/1.4802450>

View Table of Contents: <http://apl.aip.org/resource/1/APPLAB/v102/i15>

Published by the AIP Publishing LLC.

Additional information on *Appl. Phys. Lett.*

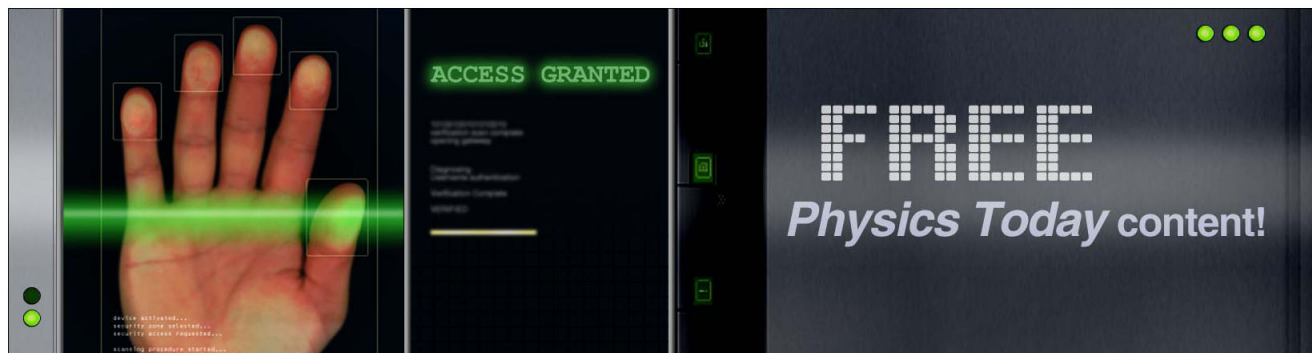
Journal Homepage: <http://apl.aip.org/>

Journal Information: http://apl.aip.org/about/about_the_journal

Top downloads: http://apl.aip.org/features/most_downloaded

Information for Authors: <http://apl.aip.org/authors>

ADVERTISEMENT



Enhanced direct flexoelectricity in paraelectric phase of Ba(Ti_{0.87}Sn_{0.13})O₃ ceramics

Longlong Shu, Xiaoyong Wei,^{a)} Li Jin,^{b)} Yong Li, Hong Wang, and Xi Yao

Electronic Materials Research Laboratory, Key Laboratory of the Ministry of Education and International Center for Dielectric Research, Xi'an Jiaotong University, Xi'an 710049, China

(Received 28 December 2012; accepted 4 April 2013; published online 16 April 2013)

Enhanced direct flexoelectricity has been observed in paraelectric phase of Ba(Ti_{0.87}Sn_{0.13})O₃ ceramics by using a quasi-static cantilever beam system. The transverse flexoelectric coefficient was found to be about 53 $\mu\text{C}/\text{m}$ near the Curie temperature. Temperature-dependence of the transverse flexoelectric coefficient was studied, exhibiting a nonlinear relationship with dielectric constant. © 2013 AIP Publishing LLC [<http://dx.doi.org/10.1063/1.4802450>]

Recently, flexoelectric effect based on inhomogeneous electrical fields or mechanical strains has attracted considerable interests due to its potential sensing applications.^{1–3} The direct flexoelectric effect is characterized by a fourth rank tensor, referred as direct flexoelectric coefficient, which relates the electric polarization vector to the strain gradient tensor.^{4,5} For dielectric materials, flexoelectricity could be found in all 32 point groups, in principle, which greatly enhance the possibility of finding attractive sensing/actuating solid materials without symmetry restriction.⁶ Although theoretical studies, focusing on the flexoelectric origin,^{5,7,8} mechanism,^{9–13} and classification¹⁴ (bulk/surface effect) of such a coupling effect, have been significantly developed in recent years, experimental studies are rather limited, especially in bulk dielectrics.^{15,16}

As suggested by Tagantsev,⁴ the theoretical estimation of flexoelectric coefficient μ is proportional to the dielectric susceptibility χ , as follows:

$$\mu \approx \gamma \chi \frac{q}{a}, \quad (1)$$

where γ is a constant value close to unity, q is the electron charge, and a is the unit cell dimension. The ratio of q/a is on the order of 10^{-10} C/m, which is a rather weak signal to be detected experimentally.¹ Ferroelectric materials are good candidates for flexoelectric effect study due to their high permittivity as high as few tens of thousand in the vicinity of the Curie temperature (T_C). Ma and Cross have systematically investigated the flexoelectric effects in various perovskites ferroelectric ceramics, such as lead magnesium niobate (PMN),^{17,18} barium strontium titanate (BST),¹⁹ lead zirconate titanate (PZT),²⁰ barium titanate (BT)²¹ through dynamic and static measurements. Different from Pb-based systems, Ba-based perovskites show much higher performance in their paraelectric phase.¹⁶

In the work of Ma and Cross,¹⁷ μ_{12} is used to describe the transverse flexoelectric effect, however, such a μ_{12} , defined as one component of a 6×6 matrix, cannot properly express the relation between induced polarization and applied strain gradient. In sense of physics, the polarization

(the subscript i) is an electrical quantity, which is not commutative with the gradient axis (the subscript l), so taking the subscript l and i as a whole to describe the effect may conflict with its physical implication. In principle, the four subscripts i, j, k, l of flexoelectric coefficients have 54 different combinations. Therefore, the direct flexoelectric coefficients are preferred to be rewritten in a 3×18 matrix form rather than 6×6 matrix form, different with electrostriction coefficients and stiffness/compliance matrixes.⁶ Let

$$\frac{\partial S_{jk}}{\partial x_l} = e_{jkl} = e_n \quad (n = 1 - 18). \quad (2)$$

The detailed definition of e_n can be found in Eq. (10) of Ref. 6. Hereafter, μ_{14} is used to describe the transverse flexoelectric effect through the following equation:

$$P_3 = \mu_{3113} \frac{\partial S_{11}}{\partial x_3} = \mu_{14} \frac{\partial S_{11}}{\partial x_3}. \quad (3)$$

Precisely, the contribution induced by the strain gradient S_{22} and S_{33} along x_3 direction should be considered for transverse mode, even though these values are relatively small compared to the strain gradient S_{11} along x_3 direction. Thus, the measured transverse flexoelectric coefficient, in principle, should be given by

$$P_3 = \mu_{11} \frac{\partial S_{33}}{\partial x_3} + \mu_{14} \left(\frac{\partial S_{11}}{\partial x_3} + \frac{\partial S_{22}}{\partial x_3} \right) = [\alpha \mu_{11} + (1 + \alpha) \mu_{14}] \frac{\partial S_{11}}{\partial x_3} = \mu_{\text{eff}} \frac{\partial S_{11}}{\partial x_3}. \quad (4)$$

Here, μ_{eff} is the effective transverse coefficient and α is the Poisson ratio in isotropic crystals. The previous experimental results^{17–21} on the bending beam mode should be associated with coefficient μ_{eff} .

The maximum μ_{eff} (100 $\mu\text{C}/\text{m}$) was observed in (Ba_{0.67}Sr_{0.33})TiO₃ (BST33) ceramic at its paraelectric state (23 °C, 2 °C above its T_C).¹⁹ The reason of this extraordinary enhancement is not clear yet. It is not simply due to high permittivity since Pb-based perovskites exhibit much lower μ_{eff} in spite of their high permittivity (20 000).²⁰ The aim of the present work is to identify the flexoelectric properties in Ba(Ti,Sn)O₃ (BTS) ceramics, where the permittivity can be high at room temperature with a proper Ti/Sn ratio.²³

^{a)}Electronic mail: wdy@mail.xjtu.edu.cn.

^{b)}Electronic mail: ljin@mail.xjtu.edu.cn.

BTS ceramic was synthesized by a conventional solid state process, as described in Ref. 22. The ceramic samples with nominal composition $\text{Ba}(\text{Ti}_{0.87}\text{Sn}_{0.13})\text{O}_3$ were labeled as BTS13. Pure perovskite structure was identified by x-ray diffraction for both calcinated and sintered bodies. Dense samples (relative density of 97%) were cut into bars ($40 \times 6 \times 1.5 \text{ mm}^3$) to fulfill the prerequisite for using the cantilever beam configuration at quasi-static condition, where the measuring frequency is far below the resonant frequency of the cantilever beam.

The framework of our μ_{eff} measurement is similar to that of Ma and Cross.^{16,17} The driving force generated by a loudspeaker (RH-603, DERVEL) was controlled by a power amplifier (HSA 4014, NF) and the output signals were collected by a lock-in amplifier (7280, SR). The strain gradient was calculated from the deflection of the ceramic samples, which was determined by a noncontact optical sensor (MTI2000, MTI). Rectangular top and bottom electrodes (area $A = 20 \text{ mm}^2$) were brushed at the center of the ceramic bar ($x_1/l = 0.5$). In our system, the ceramic sample was clamped rigidly by screw. The link between the ceramic bar and the loudspeaker is a rigid arm. In order to eliminate the polarization contribution induced by temperature gradient (inhomogeneous pyroelectric effect), at each measuring temperature, 10 min duration was kept before every measurement.

Then the same BTS13 bar was used to evaluate the system noise level. In order to exclude the signal induced by bending through the direct flexoelectric effect, the signal was collected without bending the BTS13 bar. In this case, the main signal comes from the system noise current. As shown in Fig. 1, both the noise current i and the equivalent induced polarization $P = i/\omega A$ are shown as a function of frequency. The test frequency in the previous work¹⁷ was set as 1 Hz to fulfill the quasi-static condition, in which the strain gradient calculation is only suitable and accurate. The equivalent noise polarization decreases rapidly with frequency, a higher measurement frequency could eliminate such kind noise contribution to the signal. A dummy Al_2O_3 bar with the same geometrical dimensions was further used to verify the test reliability. In this measurement, we applied a strain gradient

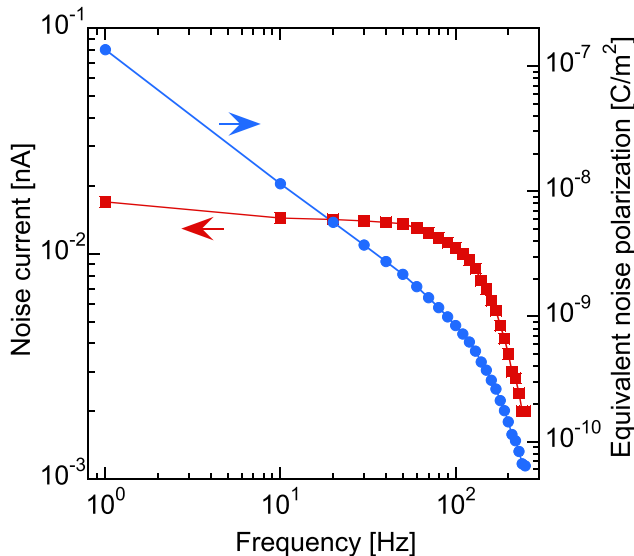


FIG. 1. Noise current and equivalent polarization as a function of frequency.

to the sample through the loudspeaker and detected the signals from it. A frequency-independent noise current with a level of $\sim 0.01 \text{ nA}$ was observed. Since in this dummy sample, the flexoelectric effect, i.e., coupling effect between the polarization and strain gradient is very weak. Only the mechanical vibration, which was introduced into measurement system by the loudspeaker, is the main source of the noise current and cannot be absolutely eliminated through the electromagnetic shielding. Fortunately, the signals detected in BTS13 under bending condition at 30 Hz possess a much higher level output (typically about 1 nA), which is two orders of magnitude higher than the noise level ($\sim 0.01 \text{ nA}$). These factors ensure the test reliability of our measurement.

The strain gradient is calculated by quasi-static mechanical vibration of cantilever beam. Based on a typical neutral plane assumption,¹⁷ the transverse strain gradient along thickness direction can be written as

$$\frac{\partial S_{11}}{\partial x_3} = -\frac{\partial^2 W(x_1)}{\partial x_1^2}, \quad (5)$$

where $W(x_1)$ is the vertical displacement in point x_1 of the beam. The mathematical solution of $W(x_1)$ is a superposition of different deformation modes. Each mode shape can be expressed as

$$W_r(x_1) = A_r[(\sin \beta_r l - \sinh \beta_r l)(\sin \beta_r x_1 - \sinh \beta_r x_1) + (\cos \beta_r l - \cosh \beta_r l)(\cos \beta_r x_1 - \cosh \beta_r x_1)], \quad (6)$$

where $A_r = C_1/(\sin \beta_r l - \sinh \beta_r l)$, $r = 1, 2, \dots$. C_1 was determined from the deflection at the electrode position.¹⁶ In order to simplify the calculation, normally we only consider the basic harmonic mode ($n = 1$). For this mode, $\beta_1 l = 1.875$. Then the resonant frequency f_1 is expressed as

$$f_1 = \frac{ck}{2\pi l^2}(\beta l)^2, \quad (7)$$

where $l = 40 \text{ mm}$, $k^2 = h^2/12$ (h is the thickness of the beam and $= 1.5 \text{ mm}$), and wave velocity c is about 3000 m/s. We found that $f_1 \approx 600 \text{ Hz}$. The testing frequency of 30 Hz is far below the resonance frequency, therefore, the quasi-static condition is hold for our measurement.

Weak-field permittivity ϵ' ($\epsilon' = \chi - 1$) and loss tangent ($\tan \delta = \epsilon''/\epsilon'$) as a function of temperature for BTS13 at different frequencies (1, 10, 100, 1000 kHz) are present in Fig. 2. A non-shifting, slightly frequency dispersive dielectric peak (20°C) indicates non-relaxor ferroelectric behavior²⁴ and the absence of local spontaneous polarization above Curie temperature. The peak value of the permittivity of BTS13 at 1 kHz is about 15 000, a bit lower than that of BST33 (18 000).¹⁹

As shown in Fig. 3, there are highly correlated linear relationships between the induced flexoelectric polarization and the strain gradient for BTS13 in the paraelectric temperature range from 24°C to 43°C . Flexoelectric coefficients can be calculated from the slopes in the strain gradient range ($1.95\text{--}2.55 \times 10^{-2} \text{ m}^{-1}$), and the largest μ_{eff} was calculated to be $53 \mu\text{C/m}$ at 24°C (4°C above T_C). The high linearity between the strain gradient and induced polarization proves

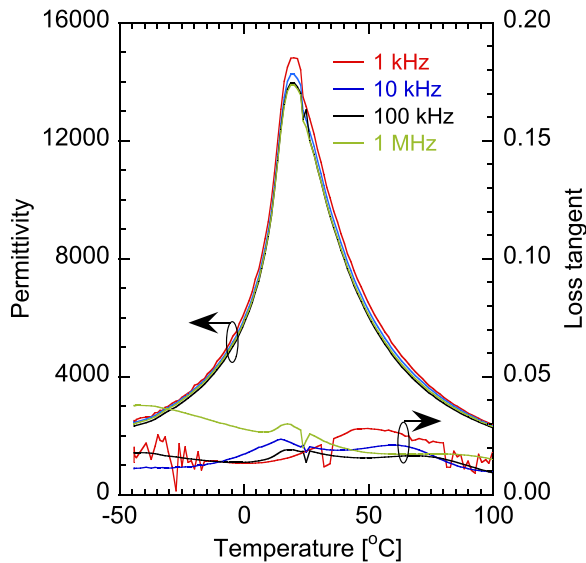


FIG. 2. Weak-field permittivity and loss tangent of BTS13 ceramic bar as a function of temperature at different frequencies.

that the existence of flexoelectric effect. The non-zero intercepts indicate the possible deviation of zero strain position.

The calculated μ_{eff} decreases gradually with temperature above T_C , which is similar to the previous reports.^{17,19–21} The permittivity dependence of μ_{eff} is shown in Fig. 4, where a near linear relationship can be seen for $\epsilon < 10000$, then the value increases dramatically with permittivity. Such an abrupt enhancement, observed in different materials,^{17,19,21} can be attributed to the instability of the crystal structure, where local polarization can be readily induced by an external strain gradient, especially in the highly polarizable matrix at temperature slightly above T_C .

Based on the above experiments, high transverse flexoelectric coefficient ($53 \mu\text{C}/\text{m}$) is observed in BTS system, which is comparative to that value ($100 \mu\text{C}/\text{m}$) reported in

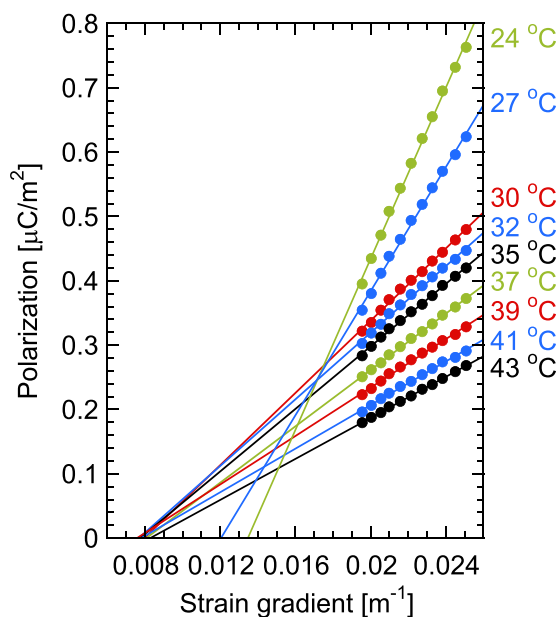


FIG. 3. Transverse flexoelectric polarization of BTS13 ceramic bar in cantilever beam framework as a function of strain gradient from 24°C to 43°C at 30 Hz. The solid lines presented in this figure are based on a linear fitting.

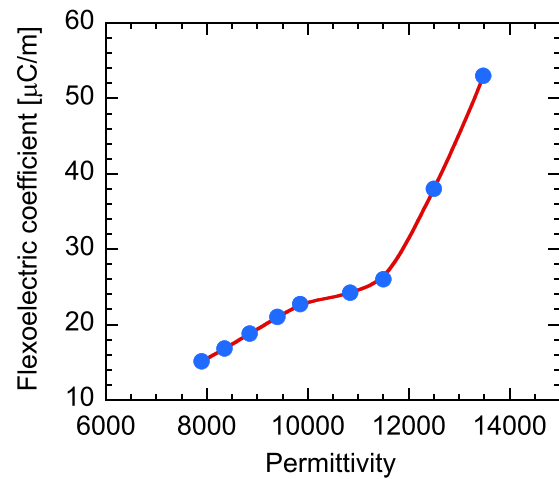


FIG. 4. Transverse flexoelectric coefficient μ_{eff} of BTS13 ceramic bar as a function of permittivity above the T_C . The solid line is a guide to the eye.

BST system.¹⁹ The validation of flexoelectricity is favored by the highly linearity between polarization and gradient as well as the low noise level. Since the ferroelectricity of BaTiO_3 mainly correlates to the coupling between Ti and O ions, the B-site substitution of Ti ion by Sn^{4+} weakens this coupling effect. With the increasing of Sn ion concentration, there is a progressive crossover from normal ferroelectric state to relaxor ferroelectric state. BTS13 can be regarded as an initial state for this structure transformation. While the substitution of Sr on A-site does not weaken the coupling effect, except for introducing oxygen octahedron tilting caused by relatively smaller radius. When the more than 80% Ba is substituted by the Sr ion in BaTiO_3 , typical relaxor ferroelectric characteristics was reported according to the evidence reflected the permittivity as a function of the temperature measured at different frequencies. This relaxor behavior is considered as a fluctuation by the Ba ion to the host quantum paraelectric SrTiO_3 .^{25,26} The relatively lower flexoelectric coefficient in BTS13 may come from such a structure difference.

Combining our data and the previous data, it can be seen that the high flexoelectric properties reported in Ba-based systems are very sensitive to temperature and maximum flexoelectric coefficients are only observed near the paraelectric-ferroelectric phase transition region. From the point view of application, a system with a broad dielectric peak at T_C would benefit a good temperature stability of such an effect. In the ferroelectric ceramics, the grain size effect and doping effect on the dielectric properties have been clearly revealed.^{27,28} As reflected through the temperature-dependent permittivity, by decreasing the grain size of BaTiO_3 ceramics from micron to nanometer scale, the permittivity peak value at T_C shows a decrease accompanied with a broadness of the peak. The grain size can also be decreased by introducing dopant into the lattice.^{29–31} If we can broaden the ferroelectric-paraelectric peak of BTS ceramics through such a grain size effect, a large flexoelectric response with good temperature stability may be expected.

In conclusion, enhanced flexoelectric coefficient is observed in barium stannate titanate ceramics. The high permittivity seems playing a significant role to the enhancement

of flexoelectricity, even the flexoelectric coefficient is non-linear with dielectric permittivity in the vicinity of phase transition point.

L.S. and L.J. gratefully acknowledge multiple discussions with Dr. Fei Li. This work was supported by National Basic Research Program of china (2009CB623306), International Science & Technology Cooperation Program of China (2013DFR50470), and National Nature Science Foundation of China (50872107 and 10875095).

- ¹L. E. Cross, *J. Mater. Sci.* **41**, 53 (2006).
- ²W. Huang, K. Kim, S. Zhang, F. G. Yuan, and X. Jiang, *Phys. Status Solidi (RRL)* **5**, 350 (2011).
- ³W. Huang, X. Yan, S. R. Kwon, S. Zhang, F. G. Yuan, and X. Jiang, *Appl. Phys. Lett.* **101**, 252903 (2012).
- ⁴A. K. Tagantsev, *Sov. Phys. JETP* **61**, 1246 (1985).
- ⁵A. K. Tagantsev, *Phys. Rev. B* **34**, 5883 (1986).
- ⁶L. Shu, X. Wei, T. Pang, X. Yao, and C. Wang, *J. Appl. Phys.* **110**, 104106 (2011).
- ⁷A. K. Tagantsev, *Phase Transitions* **35**, 119 (1991).
- ⁸R. Maranganti and P. Sharma, *Phys. Rev. B* **80**, 054109 (2009).
- ⁹M. Majdoub, P. Sharma, and T. Cagin, *Phys. Rev. B* **77**, 125424 (2008).
- ¹⁰P. Zubko, G. Catalan, A. Buckley, P. R. L. Welche, and J. F. Scott, *Phys. Rev. Lett.* **99**, 167601 (2007).
- ¹¹P. Zubko, G. Catalan, A. Buckley, P. R. L. Welche, and J. F. Scott, *Phys. Rev. Lett.* **100**, 199906 (2008).
- ¹²A. N. Morozovska, E. A. Eliseev, G. S. Svechnikov, and S. V. Kalinin, *Phys. Rev. B* **84**, 045402 (2011).
- ¹³A. K. Tagantsev and A. S. Yurkov, *J. Appl. Phys.* **112**, 044103 (2012).
- ¹⁴R. Resta, *Phys. Rev. Lett.* **105**, 127601 (2010).
- ¹⁵W. Ma, *Phys. Status Solidi B* **245**, 761 (2008).
- ¹⁶W. Ma, *Phys. Status Solidi B* **247**, 213 (2010).
- ¹⁷W. Ma and L. E. Cross, *Appl. Phys. Lett.* **78**, 2920 (2001).
- ¹⁸W. Ma and L. E. Cross, *Appl. Phys. Lett.* **79**, 4420 (2001).
- ¹⁹W. Ma and L. E. Cross, *Appl. Phys. Lett.* **81**, 3440 (2002).
- ²⁰W. Ma and L. E. Cross, *Appl. Phys. Lett.* **82**, 3293 (2003).
- ²¹W. Ma and L. E. Cross, *Appl. Phys. Lett.* **88**, 232902 (2006).
- ²²Note that the coefficients come from the definition of the flexoelectric tensor in matrix form. In high symmetry crystals, such as $m3m$ and 432, the non-zero independent components are $\mu_{1111} = \mu_{2222} = \mu_{3333} = \mu_{11}$, $\mu_{1133} = \mu_{2233} = \mu_{1122} = \mu_{2121} = \mu_{3232} = \mu_{3131} = \mu_{1(11)}$, and $\mu_{1221} = \mu_{1331} = \mu_{2112} = \mu_{2332} = \mu_{3223} = \mu_{3113} = \mu_{14}$.
- ²³X. Wei, Y. Feng, L. Hang, S. Xia, L. Jin, and X. Yao, *Mater. Sci. Eng., B* **120**, 64 (2005).
- ²⁴A. A. Bokov and Z. G. Ye, *J. Adv. Dielectr.* **2**, 1241010 (2012).
- ²⁵H. Abdelkefi, H. Khemakhem, G. Velu, J. C. Carru, and R. Von der Muhll, *J. Alloys Compd.* **399**, 1 (2005).
- ²⁶L. Zhou, P. M. Vilarinho, and J. L. Baptista, *J. Eur. Ceram. Soc.* **19**, 2015 (1999).
- ²⁷K. Kinoshita and A. Yamaji, *J. Appl. Phys.* **47**, 371 (1976).
- ²⁸G. Arlt, D. Hennings, and G. de With, *J. Appl. Phys.* **58**, 1619 (1985).
- ²⁹V. Porokhonsky, L. Jin, and D. Damjanovic, *Appl. Phys. Lett.* **94**, 212906 (2009).
- ³⁰L. Jin, Z. B. He, and D. Damjanovic, *Appl. Phys. Lett.* **95**, 012905 (2009).
- ³¹L. Jin, V. Porokhonsky, and D. Damjanovic, *Appl. Phys. Lett.* **96**, 242902 (2010).